Inorg. Chem. **2004**, *43*, 7832–7843

Influence of Terpyridine as π-Acceptor Ligand on the Kinetics and Mechanism of the Reaction of NO with Ruthenium(III) Complexes

Almut Czap, Frank W. Heinemann, and Rudi van Eldik*

Institute for Inorganic Chemistry, University of Erlangen-Nürnberg, Egerlandstr. 1, 91058 Erlangen, Germany

Received September 9, 2003

The kinetics of the unusually fast reaction of *cis*- and *trans*-$[Ru(terpy)(NH_3)_2Cl]^{2+}$ (with respect to NH_3; terpy = 2,2′:6′,2″-terpyridine) with NO was studied in acidic aqueous solution. The multistep reaction pathway observed for both isomers includes a rapid and reversible formation of an intermediate Ru^{III}–NO complex in the first reaction step, for which the rate and activation parameters are in good agreement with an associative substitution behavior of the Ru^{III} center (*cis* isomer, $k_1 = 618 \pm 2\ M^{-1}\ s^{-1}$, $\Delta H^{\ddagger} = 38 \pm 3$ kJ mol^{-1}, $\Delta S^{\ddagger} = -63 \pm 8$ J K^{-1} mol^{-1}, $\Delta V^{\ddagger} = -17.5 \pm 0.8$ cm^3 mol^{-1}; $k_{-1} = 0.097 \pm 0.001\ s^{-1}$, $\Delta H^{\ddagger} = 27 \pm 8$ kJ mol^{-1}, $\Delta S^{\ddagger} = -173 \pm 28$ J K^{-1} mol^{-1}, $\Delta V^{\ddagger} = -17.6 \pm 0.5$ cm^3 mol^{-1}; trans isomer, $k_1 = 1637 \pm 11\ M^{-1}\ s^{-1}$, $\Delta H^{\ddagger} = 34 \pm 3$ kJ mol^{-1}, $\Delta S^{\ddagger} = -69 \pm 11$ J K^{-1} mol^{-1}, $\Delta V^{\ddagger} = -20 \pm 2$ cm^3 mol^{-1}; $k_{-1} = 0.47 \pm 0.08\ s^{-1}$, $\Delta H^{\ddagger} = 39 \pm 5$ kJ mol^{-1}, $\Delta S^{\ddagger} = -121 \pm 18$ J K^{-1} mol^{-1}, $\Delta V^{\ddagger} = -18.5 \pm 0.4$ cm^3 mol^{-1} at 25 °C). The subsequent electron transfer step to form Ru^{II}–NO^+ occurs spontaneously for the *trans* isomer, followed by a slow nitrosyl to nitrite conversion, whereas for the *cis* isomer the reduction of the Ru^{III} center is induced by the coordination of an additional NO molecule (*cis* isomer, $k_2 = 51.3 \pm 0.3\ M^{-1}\ s^{-1}$, $\Delta H^{\ddagger} = 46 \pm 2$ kJ mol^{-1}, $\Delta S^{\ddagger} = -69 \pm 5$ J K^{-1} mol^{-1}, $\Delta V^{\ddagger} = -22.6 \pm 0.2$ cm^3 mol^{-1} at 45 °C). The final reaction step involves a slow aquation process for both isomers, which is interpreted in terms of a dissociative substitution mechanism (*cis* isomer, $\Delta V^{\ddagger} = +23.5 \pm 1.2$ cm^3 mol^{-1}; *trans* isomer, $\Delta V^{\ddagger} = +20.9 \pm 0.4$ cm^3 mol^{-1} at 55 °C) that produces two different reaction products, viz. $[Ru(terpy)(NH_3)(H_2O)NO]^{3+}$ (product of the *cis* isomer) and *trans*-$[Ru(terpy)(NH_3)_2(H_2O)]^{2+}$. The π-acceptor properties of the tridentate N-donor chelate (terpy) predominantly control the overall reaction pattern.

Introduction

The chemistry of nitric oxide (NO) is relevant for the environment, immune defense systems, and a wide range of physiological processes, such as neural transmission, cytotoxicity, and blood pressure regulation,[1] and is also implicated in a number of diseases (cancer, epilepsy, diabetes, arthritis, etc.).[2] This has stimulated intense drug research and development related to NO.

The ability of transition metal complexes to both scavenge and release NO has generated new interest in such complexes as metallopharmaceuticals.[3] Ruthenium has a well documented affinity for NO,[4–6] and several complexes of this metal with coordinated NO have therapeutic use in different medical applications, i.e., in the treatment of sepsis (toxic shock)[7] or in the control of high blood pressure (vasodilatation).[8] Consequently, the coordination and mechanistic chemistry of complexes that trap and/or release this remarkable molecule are of considerable interest.[9] Common characteristics of $\{Ru^{II}NO^+\}^6$ nitrosyl complexes are their octahedral stereochemistry and the presence of an extremely

* To whom correspondence should be addressed. E-mail: vaneldik@chemie.uni-erlangen.de.

(1) Feelisch, M. S.; Stamler, J. S. *Methods in Nitric Oxide Research*; John Wiley & Sons: Chichester, U.K., 1996.
(2) Fricker, S. P. *Platinum Met. Rev.* **1995**, *39*, 150.
(3) Clarke, M. J. *Coord. Chem. Rev.* **2003**, *236*, 209.
(4) Bottomley, F. *Coord. Chem. Rev.* **1978**, *26*, 7.
(5) Richter-Addo, G.-B.; Legzdins, P. *Metal Nitrosyls*; Oxford University Press: New York, 1992.
(6) Hayton, T. W.; Legzdins, P.; Sharp, W. B. *Chem. Rev.* **2002**, *102*, 935.
(7) Fricker, S. P.; Slade, E.; Powell, N. A.; Vaughn, O. J.; Henderson, G.; Murrer, S. A.; Megson, I. C.; Bisland, S. K.; Flitney, F. W. *Br. J. Pharmacol.* **1997**, *122*, 1441.
(8) Lang, D. R.; Davies, J. A.; Lopes, L. G. F.; Ferro, A. A.; Vasconcellos, L. C. G.; Franco, D. W.; Tfouni, E.; Wieraszko, A.; Clarke, M. J. *Inorg. Chem.* **2000**, *39*, 2294. Slocik, J. M.; Ward, M. S.; Somayajula, K. V.; Shepherd, R. E. *Transition Met. Chem.* **2001**, *26*, 351. Slocik, J. M.; Ward, M. S.; Shepherd, R. E. *Inorg. Chim. Acta* **2001**, *317*, 290.

10.1021/ic0350685 CCC: $27.50
Published on Web 11/05/2004

Scheme 1

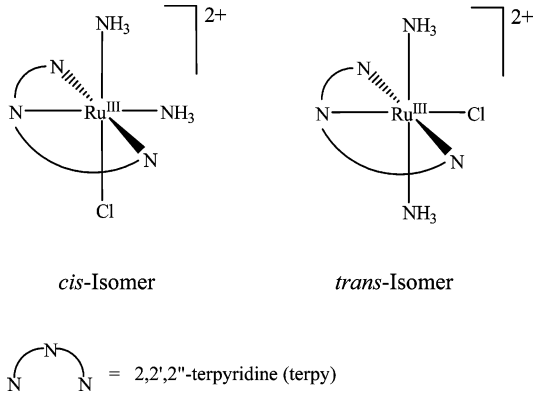

stable Ru−NO group. In general, the $\{Ru^{II}NO^{+}\}^6$ complex is formed either by reaction of Ru^{III} with NO or by acidification of Ru^{II}−nitrite solutions. Although many studies deal with the redox and substitution behavior of ruthenium nitrosyls, complex formation reactions with NO and the underlying reaction mechanisms are not well understood.

The most prominent example of a $\{Ru^{II}NO^{+}\}^6$ system is the $[Ru(NH_3)_5NO]^{3+}$ complex,[10] which is often cited in reviews and textbooks, because of the unusually fast substitution reaction that leads to this species.[11] An acidic solution of $[Ru(NH_3)_6]^{3+}$ is rapidly and quantitatively converted to $[Ru(NH_3)_5NO]^{3+}$ in the presence of NO. In a detailed reinvestigation,[12] we were able to show that bond formation with the entering NO nucleophile appears to be substantial in the transition state of the reaction. An associative substitution mechanism coupled to a concerted electron transfer process to produce $[Ru^{II}(NH_3)_5(NO^{+})]^{3+}$ was proposed to account for the rapid process.

The affinity of transition metal ions for nucleophiles such as NO can be modified by a systematic variation of the π-bonding character of the spectator ligands. π-Acceptor effects have been shown to play an important role in the substitution behavior of Pt^{II} complexes:[13] the higher the π-acceptor ability of the spectator ligand, the more electrophilic the metal center, and the higher its reactivity. The enhanced reactivity is accounted for in terms of π-backbonding from the metal to the empty π*-orbitals of the π-acceptor ligand. Because of this analogy, we investigated the effect of the displacement of ammine ligands in the earlier studied pentaammine complexes by a strong π-accepting tridentate N-donor chelate, 2,2′:6′,2″-terpyridine (terpy), on their thermodynamic and kinetic behavior. The terpy ligand coordinates meridionally in most Ru complexes and enables the formation of two isomers, viz. *cis*- and *trans*-$[Ru(terpy)(NH_3)_2Cl](PF_6)_2$ (see Scheme 1). On the basis of our earlier experience with substitution reactions of NO with different metal complexes[14] and the previous study on the unusually fast reactions between $[Ru^{III}(NH_3)_5X]^{(3-n)+}$ ($X^{n-} = Cl^-$, NH_3, H_2O) and NO,[12] we investigated the effect of the terpy ligand in *cis*- and *trans*-$[Ru(terpy)(NH_3)_2Cl]^{2+}$ on the complex formation reactions with NO. We report here the synthesis and spectroscopic and structural characterization of the *cis* and *trans* isomers of $[Ru(terpy)(NH_3)_2Cl](PF_6)_2$ and present a detailed account of the kinetics and mechanism of the reaction with NO, and the formation of two quite different reaction products in a multistep reaction sequence.

Experimental Section

Materials. $RuCl_3$ was purchased from Alfa Aesar. The ligand 2,2′:6′,2″-terpyridine (terpy), $NaPF_6$, and hydrazine hydrate were obtained from Sigma Aldrich. All solvents used in the preparative work were reagent grade and used without further purification. The synthesis of the complexes is based on the synthetically useful precursor complex $Ru(terpy)Cl_3$, which was prepared from $RuCl_3$ by the method of Meyer et al.[15] with a yield of 74%. Anal. Calcd for $Ru(terpy)Cl_3$: C 40.88; H 2.52; N 9.53. Found: C 40.91; H 2.48; N 9.73%.

Preparation of *cis*- and *trans*-$[Ru(terpy)(NH_3)_2Cl](PF_6)_2$: $Ru(terpy)Cl_3$ (200 mg, 0.45 mmol) was suspended in 50 mL of 4:1 ethanol−water, and the mixture was heated under reflux for 2 h in the presence of hydrazine hydrate (0.028 mL, 0.9 mmol). The mixture was then cooled to room temperature, and the ethanol was removed by rotary evaporation. Hydrochloric acid was added until the violet solution became orange-red, and the mixture was chilled at 0 °C. The product was isolated by filtration, washed with ethanol and diethyl ether, and dried under vacuum (yield 70%). Anal. Calcd for $[Ru(terpy)(NH_3)_2Cl](Cl)_2$: C 37.95; H 3.61; N 14.75. Found: C 38.00; H 3.52; N 14.53%. The product was recrystallized and precipitated with 2 equiv of $NaPF_6$ (76 mg, 0.9 mmol), and the two isomers were separated by fractional crystallization. The complexes were characterized by UV−vis spectroscopy, for which the molar extinction coefficient was determined from isolated crystals (average of four determinations). The *trans* isomer was also characterized by X-ray analysis (see below). ^{1}H NMR: *cis* isomer (MeOD, δ) 8.93, 2H, d, terpy-H3′; 8.68, 2H, d, terpy-H3; 8.47, 1H, t, terpy-H4′; 7.98, 2H, t, terpy-H4; 7.45, 2H, d, terpy-H6; 7.25, 2H, t, terpy-H5; *trans* isomer (MeOD, δ) 8.94, 2H, d, terpy-H3′; 8.48, 2H, d, terpy-H3; 8.38, 2H, t, terpy-H6; 8.09, 2H, t, terpy-H4; 7.77, 3H, m, terpy-H4′-H5.

All other chemicals were of analytical reagent grade, and deionized (Millipore) water was used throughout the study. CF_3SO_3H (Alfa Aesar) and CF_3SO_3Na (Sigma Aldrich) were used to adjust the ionic strength and to control the pH of the solutions (pH = 2). All experiments were performed under strict exclusion of oxygen. Acidified solutions were deaerated for extended periods

(9) Carter, T. D.; Bettache, N.; Ogden, D. *Br. J. Pharmacol.* **1997**, *122*, 971. Ford, P. C.; Bourassa, J.; Miranda, K.; Lee, B.; Lorkovic, I.; Boggs, S.; Kudo, S.; Laverman, L. *Coord. Chem. Rev.* **1998**, *171*, 185.
(10) Armor, J. N.; Scheidegger, H. A.; Taube, H. *J. Am. Chem. Soc.* **1968**, *90*, 5928.
(11) Pell, S.; Armor, J. N. *J. Am. Chem. Soc.* **1973**, *95*, 7625.
(12) Czap, A.; van Eldik, R. *Dalton Trans.* **2003**, 665.
(13) Jaganyi, D.; Hofmann, A.; van Eldik, R. *Angew. Chem., Int. Ed.* **2001**, *40*, 1680. Hofmann, A.; Jaganyi, D.; Munro, O. Q.; Liehr, G.; van Eldik, R. *Inorg. Chem.* **2003**, *42*, 1688.
(14) Wolak, M.; Stochel, G.; Zahl, A.; Schneppensieper, T.; van Eldik, R. *J. Am. Soc. Chem.* **2001**, *123*, 9780. Laverman, L. E.; Wanat, A.; Oszajca, J.; Stochel, G.; Ford, P. C.; van Eldik, R. *J. Am. Chem. Soc.* **2001**, *123*, 285. Schneppensieper, T.; Finkler, S.; Czap, A.; van Eldik, R.; Heus, M.; Nieuwenhuizen, P.; Wreesmann, C.; Abma, W. *Eur. J. Inorg. Chem.* **2001**, 491. Schneppensieper, T.; Wanat, A.; Stochel, G.; Goldstein, S.; Meyerstein, D.; van Eldik, R. *Eur. J. Inorg. Chem.* **2001**, 2317. Schneppensieper, T.; Wanat, A.; Stochel, G.; Zahl, A.; van Eldik, R. *Inorg. Chem.* **2002**, *41*, 2565. Wanat, A.; Schneppensieper, T.; Stochel, G.; van Eldik, R.; Eckhard, B.; Wieghardt, K. *Inorg. Chem.* **2002**, *41*, 4.
(15) Sullivan, B. P.; Calvert, J. M.; Meyer, T. J. *Inorg. Chem.* **1980**, *19*, 1404. Yang, J.; Seneviratne, D.; Arbatin, G.; Andersson, A. M.; Curtis, J. C. *J. Am. Chem. Soc.* **1997**, *119*, 5329.

(in general 1 min/mL of solution) with pure N_2 before being brought in contact with the Ru^{III} complexes or NO. A stock solution of NO was prepared in a gastight syringe by degassing an acidic aqueous solution, followed by saturation with NO to a final concentration of 1.43×10^{-3} M at 25 °C. Dilutions of known concentration were prepared from this saturated solution by use of syringe techniques. NO gas was purchased from Air Liquide in a purity of at least 99.5 vol % and cleaned from trace amounts of higher nitrogen oxides such as N_2O_3 and NO_2 by passing it through an Ascarite II column (NaOH on silica gel, Sigma-Aldrich) via vacuum line techniques.

Crystal Structure Determination. A suitable single crystal was coated with protective perfluoropolyether oil and mounted on a glass fiber. Data were collected on a Bruker-Nonius KappaCCD diffractometer using Mo Kα radiation (graphite monochromator).[16] Lorentz and polarization corrections were applied. Absorption effects were corrected by a semiempirical procedure based on multiple scans using the program SADABS.[17] The structure was solved by direct methods and refined on F^2 using full-matrix least-squares techniques.[18] Scattering factors and anomalous dispersion terms were taken from International Tables for X-ray Crystallography.[19] The compound crystallizes with two water molecules per complex unit. All non-hydrogen atoms were refined anisotropically. All hydrogen atom positions were taken from a difference Fourier map but were not refined. The crystallographic data were deposited at the Cambridge Crystallographic Data Center and are available on request from the following: CCDC, 12 Union Road, Cambridge CB2 1EZ. Fax: (+44)1223-336-033. E-mail: deposit@ccdc.cam.ac.uk.

Instrumentation and Measurements. pH measurements were performed on a Metrohm 632 pH-Meter with a Mettler Toledo inLab 422 glass electrode. Calibration was done by using standard buffer solutions. The concentration of NO in solution was determined with an ISO-NOP electrode connected to an ISO-NO Mark II nitric oxide sensor from World Precision Instruments. The NO electrode consists of a membrane covered anode which selectively oxidizes NO to NO_3^- ions. The resulting current is proportional to the concentration of NO in solution. The NO electrode was calibrated daily with fresh solutions of sodium nitrite and potassium iodide according to the method suggested by the manufacturers. The calibration factor nA/μM was determined with a linear fit program.

Elemental analysis (Carlo Erba 1106) and NMR spectroscopy (Bruker Avance DPX 300) were used for chemical analysis and complex characterization. ^{1}H NMR spectra were recorded using standard procedures. The chemical shifts were calibrated against TMS. IR measurements were performed on a Perkin-Elmer 16 PC FT-IR instrument using methanol and water as solvent. UV−vis spectra were recorded on a Varian Cary 5G spectrophotometer equipped with a thermostated cell compartment using a 1 cm quartz cuvette directly attached to a round flask with a sideway gas connection. This enabled the performance of different physical or chemical operations, like bubbling the solution with NO or N_2, and the measurement of spectra under exclusion of dioxygen in the same vessel.

Kinetic measurements were performed on a BioLogic SMF-20 stopped-flow instrument connected to a J&M Tidas MCS/100-1 diode array detector by rapidly mixing solutions containing Ru^{III} and NO using the syringe control device MPS-20. Changes in absorbance were monitored at 316 nm for *cis*-$[Ru(terpy)(NH_3)_2Cl]^{2+}$ and at 325 nm for *trans*-$[Ru(terpy)(NH_3)_2Cl]^{2+}$. Rapid scan measurements were performed using a J&M-Tidas 16-416 diode-array detector connected to a SX-18MV (Applied Photophysics) thermostated (±0.1 °C) stopped-flow spectrometer coupled to an online data acquisition system. Experiments at elevated pressure (0.1−130 MPa) were performed on a laboratory-made high-pressure stopped-flow instrument.[20] All kinetic experiments were performed under pseudo-first-order conditions, and the reported rate constants are the mean values from at least five kinetic runs.

The release of chloride during the reactions with NO was monitored with an ORION chloride combination electrode model 96-17B coupled to an online data acquisition system using the program PCM 700 (ORION), which is based on the Nernst equation. The reaction was studied for [*cis*-$Ru(terpy)(NH_3)_2Cl^{2+}$] = [*trans*-$Ru(terpy)(NH_3)_2Cl^{2+}$] = 1×10^{-4} M and [NO] = 7.2×10^{-4} M at 25 °C. The final concentration of chloride detected in solution was 3.52 ppm (*cis* isomer) and 3.56 ppm (*trans* isomer), which is equivalent to the employed complex concentrations.

The release of NO^+ from the nitrosyl complexes, which under the selected experimental conditions is equivalent to the release of NO_2^-, was followed with a commercially available nitrite test procedure (Spectroquant Merck). This photometric method works in the range 0.015−3.00 mg/L NO_2^- and is based on the Griess nitrite reaction: sulfonic acid and *N*-(1-naphthyl)ethylenediammonium dichloride (NNEDDC) are coupled by nitrite to produce a violet-red azo dye absorbing at 525 nm, $\epsilon = 37.1 \times 10^3$ M^{-1} cm^{-1}. It was found that a saturated NO solution also activates the Griess reaction, and for this reason, the following procedure was adopted for the quantification of nitrite: 10 mL of a deaerated, N_2 saturated pH 2 solution was bubbled with NO for 15 min. This saturated NO solution was checked by UV−vis spectroscopy to ensure the absence of nitrite ($\lambda_{max} = 371$ nm, $\epsilon = 51$ M^{-1} cm^{-1}). Then, the solution was saturated with pure N_2 for 15 min to remove NO and subsequently tested for nitrite using the Griess reaction. This value was used as a blank in the subsequent tests. The same procedure was applied to the complex solutions ([*trans*-$Ru(terpy)(NH_3)_2Cl^{2+}$] = 2.96×10^{-5} M and [*cis*-$Ru(terpy)(NH_3)_2Cl^{2+}$] = 4.8×10^{-5} M) with the exception that after saturation with NO the complex solution was stored for another 20 min to ensure that the reaction was complete. In the case of the *cis* isomer, no meaningful change in the absorbance of the violet-red azo-dye was observed, in contrast to the *trans* isomer, where the change in absorbance due to the presence of nitrite corresponds almost to the employed complex concentration. These measurements were repeated several times to ensure the reproducibility of the procedure.

Results

Crystal Structure. The molecular structure of *trans*-$[Ru(terpy)(NH_3)_2Cl](PF_6)_2 \cdot 2H_2O$ is shown in Figure S1, Supporting Information. A summary of crystal data and structure refinement parameters is given in Table S1, and selected bond distances and angles are listed in Table S2 (all as Supporting Information). The cationic complex is monomeric. The ruthenium metal is coordinated in a distorted

(16) Duisenberg, A. J. M.; Kroon-Batenburg, L. M. J.; Schreurs, A. M. M. *J. Appl. Crystallogr.* **2003**, *36*, 220.
(17) *SADABS*; Bruker AXS, Inc.: Madison, WI, 2002.
(18) *SHELXTL 6.12*; Bruker AXS, Inc.: Madison, WI, 2002.
(19) Wilson, A. J. C. *International Tables for Crystallography*; Kluwer Academic Publishers: Dordrecht, The Netherlands, 1992; Vol C, Tables 6.1.1.4 (pp 500−502), 4.2.6.8 (pp 219−222), and 4.2.4.2 (pp 193−199).
(20) van Eldik, R.; Gaede, W.; Wieland, S.; Kraft, J.; Spitzer, M.; Palmer, D. A. *Rev. Sci. Instrum.* **1993**, *64*, 1355.

Table 1. UV−Vis Spectral Data

complex	absorption data, λ_{max}, nm ($\epsilon \times 10^{-3}$ M^{-1} cm^{-1})
trans-[Ru(terpy)$(NH_3)_2$Cl]$^{2+}$	236 (20.7), 274 (sh), 282 (24.3), 325 (17.9)
cis-[Ru(terpy)$(NH_3)_2$Cl]$^{2+}$	230 (26.6), 272 (23.4), 280 (sh), 316 (23.5), ∼360 (sh), 474 (2.3)
trans-[Ru(terpy)$(NH_3)_2(H_2O)$]$^{2+}$	236 (∼33.2), 282 (sh), 290 (∼14.9), 374 (∼9.1)
[Ru(terpy)$(NH_3)(H_2O)NO$]$^{3+}$ (product of the *cis* isomer)	230 (∼36.2), 270 (∼19.6), 278 (sh), 295 (sh), 306 (∼15.4), 314 (sh), 356 (sh), 474 (∼1.8)

octahedral arrangement by one terpy molecule in a meridional way, two ammonia molecules located *trans* to each other, and one chloride ion in the equatorial (terpy) plane. Remarkable deviations from an ideal octahedron are mainly caused by the geometrical constraints of the terpy ligand. Thus, the terpy ligand N(terminal)−Ru−N(terminal) angle N1−Ru1−N3 amounts to 157.3(2)°, while the other two *trans* angles N2−Ru1−Cl1 (176.9(1)°) and N4−Ru1−N5 (176.9(2)°) are close to the ideal value of 180°. The Ru−N(terminal) bond distances of 2.070(3) and 2.071(3) Å are longer than that of Ru−N(center) (1.993(3) Å). To a great extent, the terpy ligand is planar: the strongest deviation from a least-squares plane calculated through all its nonhydrogen atoms is 0.072(3) Å for C13. These results are in good agreement with other Ru^{III} terpyridine complexes.[21,22] The Ru−Cl distance (2.331(1) Å) lies within the range reported for other Ru^{III} terpyridine complexes.[21] For the structure of the [Ru$(NH_3)_5$Cl]$^{2+}$ complex, the Ru−Cl bond length was reported to be 2.37 Å.[23] Within the crystal lattice cations, anions and solvent water molecules are linked up by an extensive network of hydrogen bonds.

Absorption Spectra and Repetitive Scan Spectra. It is known that Ru^{III} ammine complexes undergo disproportionation in alkaline solution.[24,25] In most cases, studies on substitution reactions have been confined to acidic solutions. A pH of 2 was selected to allow a good comparison with the pentaammine complexes for the reaction with NO.[12] Both isomers show no spectral changes over the pH range $1 \leq pH \leq 3$.

The UV−vis spectral data for the two isomers and their reaction products recorded in aqueous solution are summarized in Table 1. The spectra of both isomers are compared in Figure 1. The intense UV bands arise from $\pi \rightarrow \pi^*$ intraligand-centered transitions consistent with the electron withdrawing character of terpy. Both isomers show the expected similarity in the absorption bands. The *trans* isomer displays fewer absorption bands according to the higher symmetry of the complex.

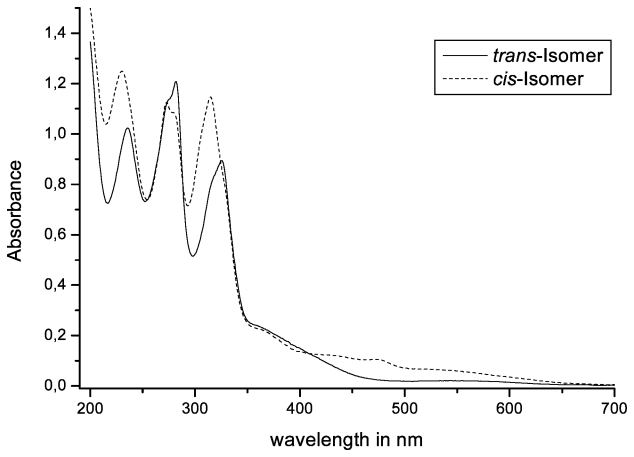

Figure 1. UV−vis absorption spectra of *cis*- and *trans*-[Ru(terpy)$(NH_3)_2$Cl]$^{2+}$ in pH 2 solution at room temperature with [*trans*-Ru(terpy)$(NH_3)_2$Cl^{2+}] = 5.0×10^{-5} M and [*cis*-Ru(terpy)$(NH_3)_2$Cl^{2+}] = 4.9×10^{-5} M.

Preliminary UV−vis and kinetic observations showed that the reaction of both isomers with NO is complex. Repetitive scan spectra for the reaction with NO were recorded in the range 200−500 nm with a total time base of 1500 s. Different time scales were adopted in order to observe the spectral changes more clearly, i.e., 10 and 1500 s for *trans*-[Ru(terpy)$(NH_3)_2$Cl]$^{2+}$, and 12, 300, and 1500 s for *cis*-[Ru(terpy)$(NH_3)_2$Cl]$^{2+}$ (see Figure 2), under kinetic conditions.After mixing the complexes with NO, there is an immediate rapid reaction as seen from the decrease in the absorbance maximum at 325 and 316 nm, respectively, indicating a multistep reaction pathway. Both isomers clearly show the same behavior for the first reaction step with the formation of several well-defined isosbestic points at 260, 288, 302, 350, and 392 nm for *trans*-[Ru(terpy)$(NH_3)_2$Cl]$^{2+}$ and 262, 339, and 387 nm for *cis*-[Ru(terpy)$(NH_3)_2$Cl]$^{2+}$. The spectra demonstrate that NO is required in excess for the first step of the reaction to proceed, which is accompanied by the formation of a new band at 374 nm for the *trans* isomer and one at ∼356 nm for the *cis* isomer.

This primary fast reaction step is followed by a subsequent second reaction which occurs on a longer time scale. In the case of *cis*-[Ru(terpy)$(NH_3)_2$Cl]$^{2+}$, the isosbestic points remain and are accompanied by a more pronounced decrease in absorbance at 316 nm and an increase at ∼356 nm. For the *trans* isomer, the rate constants of the second and third reaction step are very similar, such that it was impossible to separate the second step (Figures S2 and S3, Supporting Information). Finally, the rapid scan spectra show a third subsequent slow reaction for both isomers. The isosbestic points are shifted slightly by 3 nm to higher energy during this reaction, including a significant decrease in absorbance at 325 or 316 nm that indicates the formation of a new species.

Product Characterization. A striking feature of the infrared spectra is that the product of the *trans* isomer does not show a ν(NO) stretching band, whereas for the *cis* isomer a strong ν(NO) stretching band is observed at 1926 cm^{-1},

(21) Mondal, B.; Chakraborty, S.; Munshi, P.; Walawalkar, M. G., Lahiri, G. K. *Dalton Trans.* **2000**, 2327.
(22) Lebeau, E. L.; Adeyemi, S. A.; Meyer, T. J. *Inorg. Chem.* **1998**, *37*, 6476.
(23) John, E.; Schugar, H. J.; Potenza, J. A. *Acta Crystallogr.* **1992**, *C48*, 1574.
(24) Rudd, P. D.; Taube, H. *Inorg. Chem.* **1971**, *10*, 1543.
(25) Lay, P. A. *Comments Inorg. Chem.* **1991**, *11*, 235.

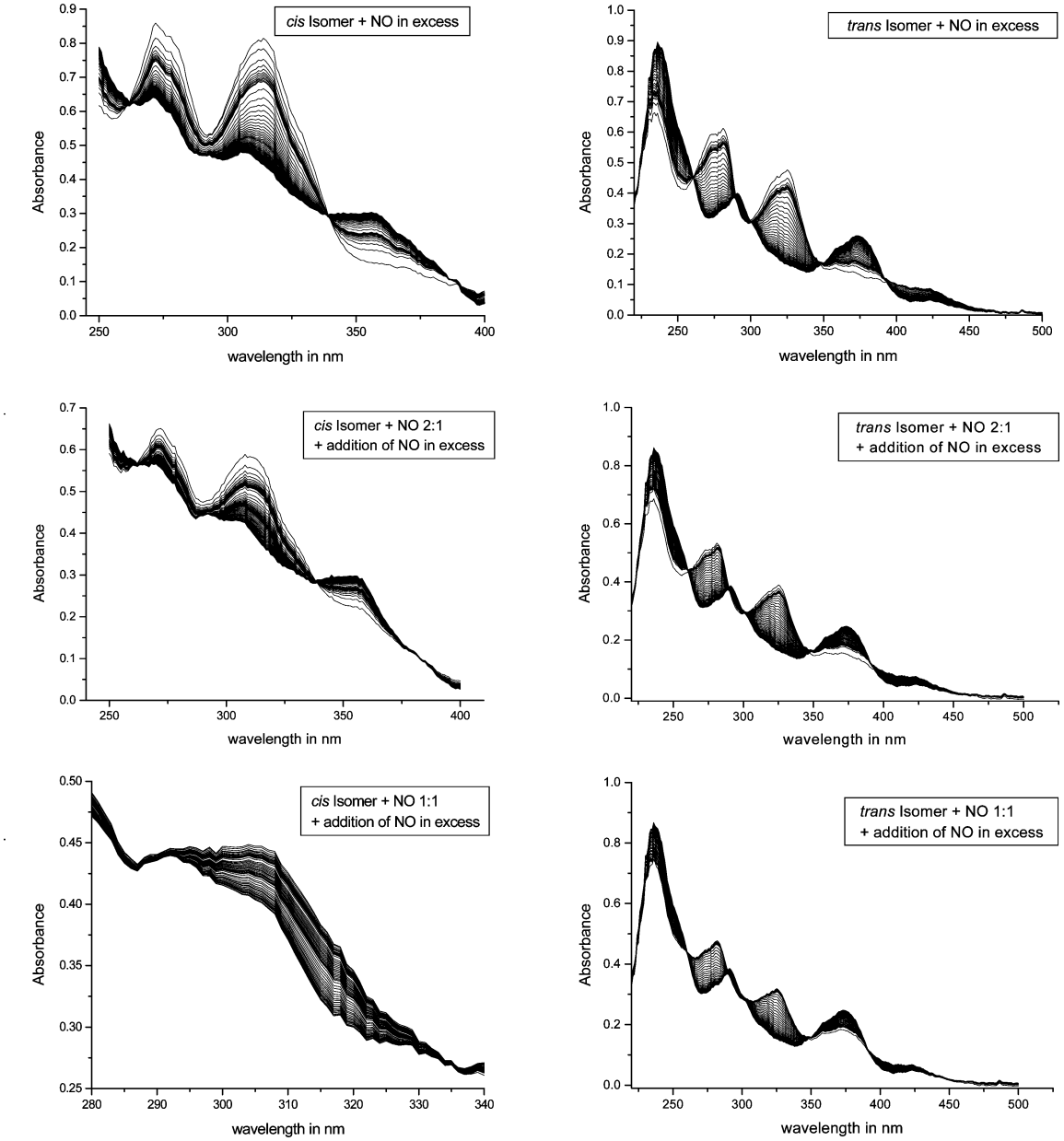

Figure 2. UV−vis spectra recorded for the reaction of *cis*- and *trans*-$[Ru(terpy)(NH_3)_2Cl]^{2+}$ with NO. Experimental conditions: $\mu = 0.1$ M, pH = 2.0, [*cis*-$Ru(terpy)(NH_3)_2Cl^{2+}$] = [*trans*-$Ru(terpy)(NH_3)_2Cl^{2+}$] = 3.15×10^{-5} M and [NO] = 0.72 mM, $T = 25$ °C. The ratio of the concentrations of both reactants [complex]/[NO] was varied from 2:1 to 1:1 mixed in a gastight syringe and after a reaction time of at least 3 h, measured again with NO in excess, [NO] = 0.72 mM. Different time scales were adopted in order to observe the spectral changes more clearly (10 and 1500 s for *trans*-$[Ru(terpy)(NH_3)_2Cl]^{2+}$, and 12, 300, and 1500 s for *cis*-$[Ru(terpy)(NH_3)_2Cl]^{2+}$).

consistent with earlier assignments for different nitrosyl−pyridyl complexes.[26,27] The relatively high infrared stretching frequencies for coordinated NO are indicative that a high degree of positive charge resides on the coordinated nitrosyl.[28] The diamagnetic character observed for nitrosyl complexes is typical for $\{RuNO\}^6$ type complexes.[29] All $\{RuNO\}^6$ complexes so far prepared are six-coordinate mono-nitrosyl complexes with an essentially linear Ru^{II}−NO^+ bond.[4]

The UV−vis spectra of the reaction products are presented in Figure 3, and the data are summarized in Table 1. The spectra clearly show that, following the reaction with NO, two significantly different reaction products are formed. A comparison with UV−vis spectral data of related complexes in the literature is inadequate because of different solvents used;[30,31] i.e., organic solvents such as CH_3CN, CH_2Cl_2, or MeOH were used to improve the solubility for particular measurements (mainly electrochemistry), often combined with the lack of such data. The $[Ru(terpy)(NH_3)(H_2O)NO]^{3+}$ complex (product of the *cis* isomer) shows spectral characteristics that fit well with general assignments made for

(26) Nagao, N.; Nishimura, H.; Funato, H.; Ichikawa, Y.; Howell, F. S.; Mukaida, M.; Kakihana, H. *Inorg. Chem.* **1989**, *28*, 3955.
(27) Hirano, T.; Ueda, K.; Mukaida, M.; Nagao, H.; Oi, T. *Dalton Trans.* **2001**, 2341.
(28) Godwin, J. B.; Meyer, T. J. *Inorg. Chem.* **1971**, *10*, 471.
(29) Enemark, J.; Feltham, R. D. *Coord. Chem. Rev.* **1974**, *13*, 339.
(30) Pipes, D. W.; Meyer, T. J. *Inorg. Chem.* **1984**, *23*, 2466.
(31) Callahan, R. W.; Meyer, T. J. *Inorg. Chem.* **1977**, *16*, 574.

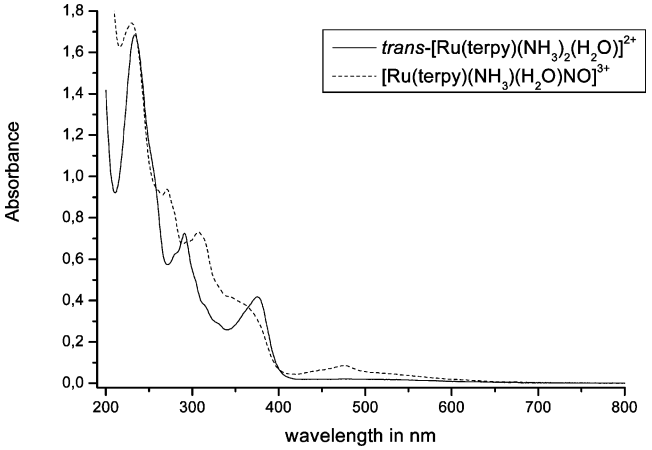

Figure 3. UV−vis absorption spectra of products of *cis*- and *trans*-[Ru(terpy)$(NH_3)_2$Cl]$^{2+}$ after the reaction with NO at pH 2 and room temperature with [*trans*-Ru(terpy)$(NH_3)_2(H_2O)^{2+}$] = ∼4.6 × 10^{-5} M, [Ru(terpy)(NH_3)-$(H_2O)NO^{3+}$] = ∼4.8 × 10^{-5} M.

nitrosyl complexes.[32−34] For the *trans*-[Ru(terpy)$(NH_3)_2$-$(H_2O)]^{2+}$ complex, we conclude on the basis of the final spectrum obtained that the high symmetry is conserved since no new bands are formed in the 400−700 nm range.

First Reaction Step. All rate constants were measured under pseudo-first-order conditions with NO in excess: [*cis*-Ru(terpy)$(NH_3)_2Cl^{2+}$] = [*trans*-Ru(terpy)$(NH_3)_2Cl^{2+}$] = 2.4 × 10^{-5} M and [NO] = 0.24−1.19 mM at pH 2. Since all the kinetic and thermodynamic data represent straight-line fits, all plots are given under Supporting Information (*trans* isomer, Figures S4−S7; *cis* isomer, Figures S8−S11). The observed rate constants measured as a function of [NO] and temperature (Figures S4 and S8) were obtained from a two-exponential fit (first and second step) of the kinetic traces (best mathematical fit to a kinetic model involving two consecutive first-order reactions). These plots exhibit a linear dependence of the observed rate constant on [NO], with a meaningful intercept pointing to a reverse or parallel reaction.

In a series of experiments, the ratio of the concentrations of both reactants [complex]/[NO] was varied from 2:1 to 4:3 and 1:1 (see Figure 2 for more details), mixed in a gastight syringe, and, after a reaction time of at least 3 h, measured again with NO in excess. For both isomers, the characteristic two-/three-step reaction pathway occurs again on addition of excess NO. It follows from these experiments that more than 1 equiv of NO is required to complete the reaction.

The rate constants for the first step were measured as a function of temperature in the range 5−25 °C for the *trans* isomer and from 12 to 32 °C for the *cis* isomer. The higher temperature range in the case of the *cis* isomer was selected as a result of precipitation that occurred when the reactants were mixed at temperatures ≤10 °C. The Eyring plots for these data (Figures S5 and S9) illustrate linear behavior within the error limits of the data, where $\Delta H^{\ddagger}$ and $\Delta S^{\ddagger}$ can be estimated from the slope and intercept, respectively.

Table 2. Activation Parameters for the Reaction of *cis*- and *trans*-[Ru(terpy)$(NH_3)_2Cl]^{2+}$ with NO

	cis-[Ru(terpy)-$(NH_3)_2Cl]^{2+}$	*trans*-[Ru(terpy)-$(NH_3)_2Cl]^{2+}$
k_1 [$M^{-1}\,s^{-1}$] at 25°C	618 ± 2	1637 ± 11
$\Delta H^{\ddagger}$ [kJ mol^{-1}]	38 ± 3	34 ± 3
$\Delta S^{\ddagger}$ [J $K^{-1}\,mol^{-1}$]	−63 ± 8	−69 ± 11
$\Delta V^{\ddagger}$ [$cm^3\,mol^{-1}$]	−17.5 ± 0.8	−20 ± 2
k_{-1} [s^{-1}] at 25 °C	0.097 ± 0.001	0.47 ± 0.08
$\Delta H^{\ddagger}$ [kJ mol^{-1}]	27 ± 8	39 ± 5
$\Delta S^{\ddagger}$ [J $K^{-1}\,mol^{-1}$]	−173 ± 28	−121 ± 18
$\Delta V^{\ddagger}$ [$cm^3\,mol^{-1}$]	−17.6 ± 0.5	−18.5 ± 0.4
K_1 (=k_1/k_{-1}) [M^{-1}] at 25 °C	6371	3520
k_2 [$M^{-1}\,s^{-1}$] at 45°C	51.3 ± 0.3	
$\Delta H^{\ddagger}$ [kJ mol^{-1}]	46 ± 2	
$\Delta S^{\ddagger}$ [J $K^{-1}\,mol^{-1}$]	−69 ± 5	
$\Delta V^{\ddagger}$ [$cm^3\,mol^{-1}$]	−22.6 ± 0.2	
k_3 [s^{-1}] at 55°C	(1.39 ± 0.04) × 10^{-2}	(2.49 ± 0.03) × 10^{-2}
$\Delta V^{\ddagger}$ [$cm^3\,mol^{-1}$]	+23.5 ± 1.2	+20.9 ± 0.4

The reactions were also studied as a function of pressure over the range 0.1−130 MPa (Figures S6 and S10), for which ln *k* appeared to be a linear function of pressure (Figures S7and S11). From the slope of the plots (=$-\Delta V^{\ddagger}$) the volume of activation, $\Delta V^{\ddagger}$, was estimated. The rate and activation parameters are summarized in Table 2, from which it follows that they are in good agreement for both isomers.

Second Reaction Step. The second reaction step was also studied under pseudo-first-order conditions with NO in excess at 45 °C: [*cis*-Ru(terpy)$(NH_3)_2Cl^{2+}$] = 2.4 × 10^{-5} M and [NO] = 0.24−1.19 mM at pH 2. Interestingly, in the case of the *trans* isomer, no dependence on [NO] could be detected. Furthermore, the second and third reaction steps overlap at 45 °C and could therefore not be separated kinetically. In order to improve the separation and determination of the rate constant k_2 for the *cis* isomer, the reaction was studied at 45 °C, since under these conditions the first reaction step is significantly accelerated and k_2 predominantly controls the kinetic trace. The kinetic traces gave best mathematical fits to a kinetic model involving two consecutive first-order reactions. Since all the kinetic data represent straight-line fits, all plots are given under Supporting Information (Figures S12 −S14). The dependence of the observed rate constant for the second step on [NO] (Figure S12) confirms that the reaction is first order in both reactants and shows no intercept, indicating that the reaction goes to completion.

The rate constant k_2 was also measured as a function of temperature in the range 25−45 °C at pH 2: [*cis*-Ru(terpy)-$(NH_3)_2Cl^{2+}$] = 2.4 × 10^{-5} M and [NO] = 1.19 mM. The Eyring plot for these data (Figure S13) demonstrates a linear behavior, where the slope represents $\Delta H^{\ddagger}$ and the intercept $\Delta S^{\ddagger}$.The reaction was also studied as a function of pressure over the range 0.1−130 MPa, for which ln k_2 appeared to be a linear function of pressure (Figure S14). From the slope of the plot, $\Delta V^{\ddagger}$ was estimated. The rate and activation parameters are summarized in Table 2.

(32) Assefa, Z.; Stanbury, D. M. *J. Am. Chem. Soc.* **1997**, *119*, 521.
(33) Bezerra, C. W. B.; da Silva, S. C.; Gambardella, M. T. P.; Santos, R. H. A.; Plicas, L. M. A.; Tfouni, E.; Franco, D. W. *Inorg. Chem.* **1999**, *38*, 5660.
(34) Tfouni, E.; Krieger, M.; McGarvey, B. R.; Franco, D. W. *Coord. Chem. Rev.* **2003**, *236*, 57.

Scheme 2. Reaction Pathway for *cis*-$[Ru(terpy)(NH_3)_2Cl]^{2+}$

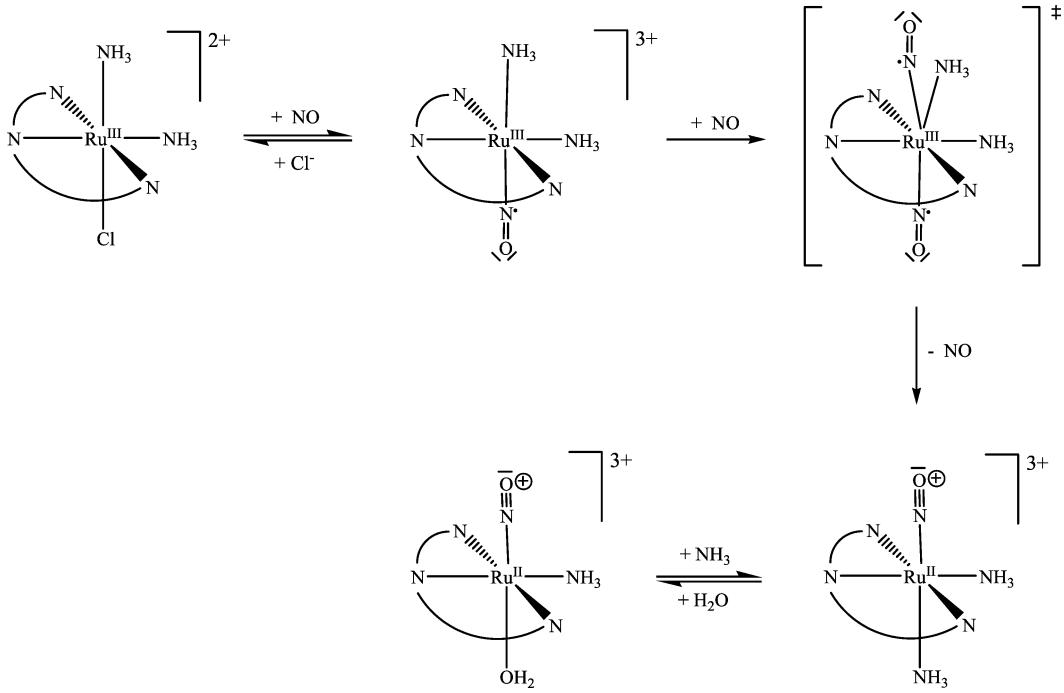

Third Reaction Step. The third step of the overall reaction for both isomers was studied at 55 °C: [*cis*-$Ru(terpy)(NH_3)_2Cl^{2+}$] = [*trans*-$Ru(terpy)(NH_3)_2Cl^{2+}$] = 2.4×10^{-5} M and [NO] = 0.24−1.19 mM at pH 2. The advantage of increasing the temperature to 55 °C is again the improved kinetic separation and determination of k_3. The first reaction step is significantly accelerated at this temperature and does not interfere in the evaluation of the rate constant k_3. The kinetic traces obtained gave best mathematical fits to a kinetic model involving two consecutive first-order reactions (second and third reaction steps) for the *cis* isomer and a first-order reaction (combined second and third reaction steps) for the *trans* isomer.

A striking feature is that the third reaction step shows no dependence on the NO concentration for both isomers, and it is therefore reasonable to assume that this step involves an aquation process. This suggestion is supported by the activation volumes determined from the pressure dependence of the observed rate constants (Figure S15, Supporting Information). The rate and activation parameters are summarized in Table 2.

On the basis of these kinetic observations, the overall reaction sequence can be formulated as shown in Schemes 2 and 3 for *cis*- and *trans*-$[Ru(terpy)(NH_3)_2Cl]^{2+}$, respectively.

Discussion

On the basis of our experience with substitution reactions of Ru^{III} ammine complexes with NO,[12] it was the goal of this study to find related systems that will enable us to gain further insight into the reaction mechanism in order to clarify the unusually high reaction rates. The overall reaction between the Ru^{III} pentaammine complexes and the direct attack of NO is presented in eq 1.

$$[Ru^{III}(NH_3)_5X]^{(3-n)+} + NO \rightarrow [Ru(NH_3)_5(NO)]^{3+} + X^{n-} \quad (1)$$

$$(X^{n-} = NH_3, H_2O, Cl^-)$$

Ru^{III} pentaammine complexes are in general substitution inert and thus undergo very slow substitution reactions with rate constants of the order of 10^{-4} M^{-1} s^{-1} at 55 °C.[35] However, these complexes show an unusually high reactivity in the reaction with NO. The measured second-order rate constant and the activation parameters determined for $[Ru(NH_3)_5Cl]^{2+}$ in reaction 1 are $k = 0.75 \pm 0.03$ M^{-1} s^{-1}, $\Delta H^{\ddagger} = 34.4 \pm 1.0$ kJ mol^{-1}, $\Delta S^{\ddagger} = -132 \pm 3$ J K^{-1} mol^{-1}, and $\Delta V^{\ddagger} = -18.0 \pm 0.5$ cm^3 mol^{-1} at 26 °C. Reaction 1 can be accounted for in terms of a unique combination of an associative nucleophilic attack by NO coupled to a concerted formal reduction of the metal center. The overall reaction behavior is predominantly controlled by ligand substitution.[36]

The incorporation of a tridentate N-donor chelate (terpy) in the coordination sphere of the ammine complexes affects not only the reactivity of the complex but also the pathways for the reaction with NO. The two synthesized complexes of $[Ru(terpy)(NH_3)_2Cl]^{2+}$ are classified as geometrical isomers; i.e., they have different chemical and physical properties that lead to different reactivities. For simplicity reasons, the above adopted separation of the overall reaction into

(35) Broomhead, J. A.; Kane-Maguire, L. *Inorg. Chem.* **1971**, *10*, 85.
(36) An outer-sphere electron transfer process cannot account for the observed kinetic data of reaction 1 as judged from the negative activation volume and the redox potential (see ref 12). Therefore, the electrochemistry of both isomers is not included in this study.

Scheme 3. Reaction Pathway for *trans*-$[Ru(terpy)(NH_3)_2Cl]^{2+}$

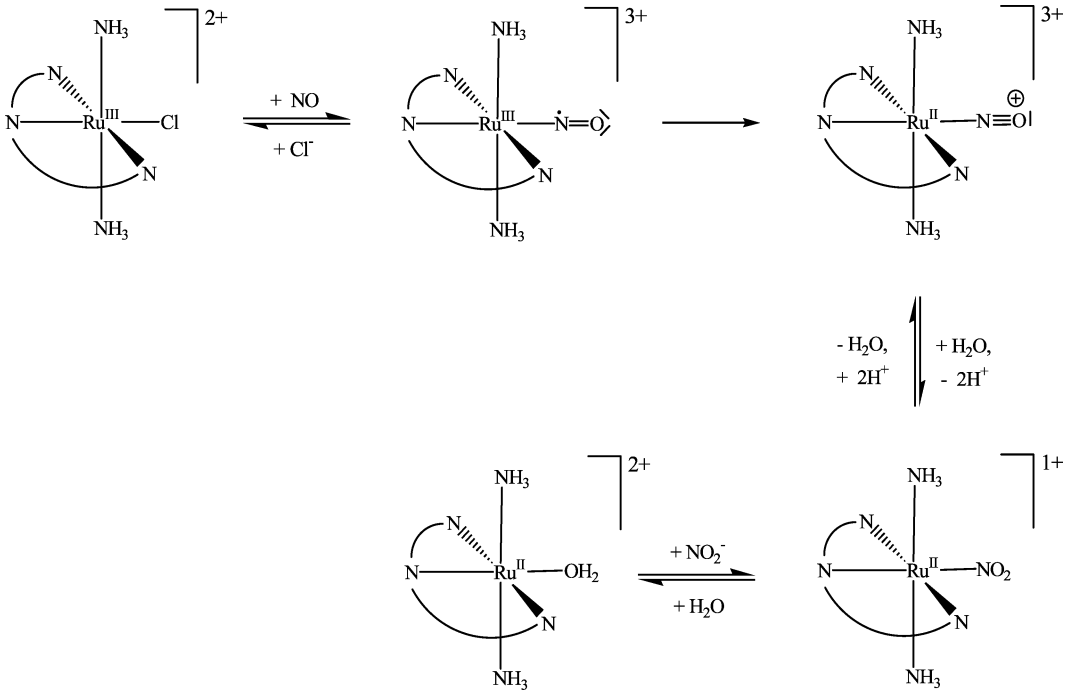

different steps will be continued in the following interpretation and discussion of the experimental observations.

First Reaction Step. Since the first reaction step is clearly similar for both isomers, no differentiation in the interpretation of the experimental data will be made. The [NO] dependence fits a rate law of the type shown in eq 2, where k_1 represents the direct attack of NO to displace the most labile ligand, viz. Cl^-, and k_{-1} describes a parallel [NO]-independent or reverse reaction.

$$k_{obs} = k_1[NO] + k_{-1} \quad (2)$$

A reverse reaction must involve the displacement of coordinated NO by Cl^- on the Ru^{III} center. In contrast, only an aquation reaction of coordinated chloride could account for a parallel reaction to form a more labile Ru^{III} aqua complex that reacts rapidly with NO in a subsequent non-rate-determining step.[37] For the aquation of $[Ru(NH_3)_5Cl]^{2+}$, the rate constant was reported to be 3.1×10^{-6} s^{-1} at 35 °C[38] and 3.28×10^{-4} s^{-1} at 80 °C.[39] In comparison to the investigated isomers, an enhanced reactivity for the aquation process is expected on the basis of the higher electrophilicity of the Ru^{III}(terpy) center. However, the measured k_{-1} values of 0.465 ± 0.080 s^{-1} (*trans* isomer) and 0.097 ± 0.001 s^{-1} (*cis* isomer) at 25 °C are larger by a factor of 10^6, which suggests that a parallel aquation reaction cannot account for the observed intercept.

The activation parameters found for the forward, [NO]-dependent reaction (k_1) are all indicative of an associative reaction mechanism (see Table 2). These data support an efficient bond formation process, accompanied by a substantial decrease in entropy and a significant volume collapse. The activation parameters for the intercept k_{-1} are of the same order of magnitude and confirm a mechanistically similar reverse reaction with chloride. This will require the equilibrium position of the first reaction step to depend on the NO concentration, which is indeed the case as judged from the overall absorbance change associated with this reaction as a function of [NO]. Under such conditions, k_{-1} will include the chloride concentration released in the forward reaction. In the rapid scan spectra, even though the ratio of the concentrations of both reactants is varied (see Figure 2), the characteristic two-/three-step reaction pathway remains, indicating that the intercept for the primary step refers to the back reaction. This is supported by other rapid scan experiments performed with a 10-fold excess of Cl^- and by using 0.01 M HCl to adjust the pH (i.e., a 400-fold excess). In both cases, the excess chloride causes an increase in k_{obs} and reduces the overall absorbance change associated with this reaction as a function of [NO].

The measured rate constants for the forward reaction are 618 ± 2 and 1637 ± 11 M^{-1} s^{-1} for *cis*- and *trans*-$[Ru(terpy)(NH_3)_2Cl]^{2+}$, respectively. By comparison with the rate constant for the reaction of $[Ru(NH_3)_5Cl]^{2+}$ with NO, the *cis* isomer exhibits an acceleration by a factor of $\sim 8 \times 10^2$ and the *trans* isomer by a factor of $\sim 2 \times 10^3$. From the substitution behavior of Pt^{II} complexes, it is well-known that the $[Pt(terpy)(L)]^{(2-n)+}$ complex shows an enhanced lability by a factor of 10^4-10^5 relative to the corresponding $[Pt(dien)(L)]^{(2-n)+}$ complex (dien = diethylenetriamine).[13] This feature is also expected for both isomers in their reaction with NO as a result of the high electrophilicity of the Ru^{III}(terpy) center caused by the strong π-acceptor properties of the terpy ligand.

(37) However, such a parallel reaction should also, at least partly, be observed in the absence of added NO, which was not the case in the present study.
(38) Anderes, B.; Collins, S. T.; Lavallee, D. K. *Inorg. Chem.* **1984**, *23*, 2201.
(39) Broomhead, J. A.; Kane-Maguire, L. *Inorg. Chem.* **1968**, *7*, 2519.

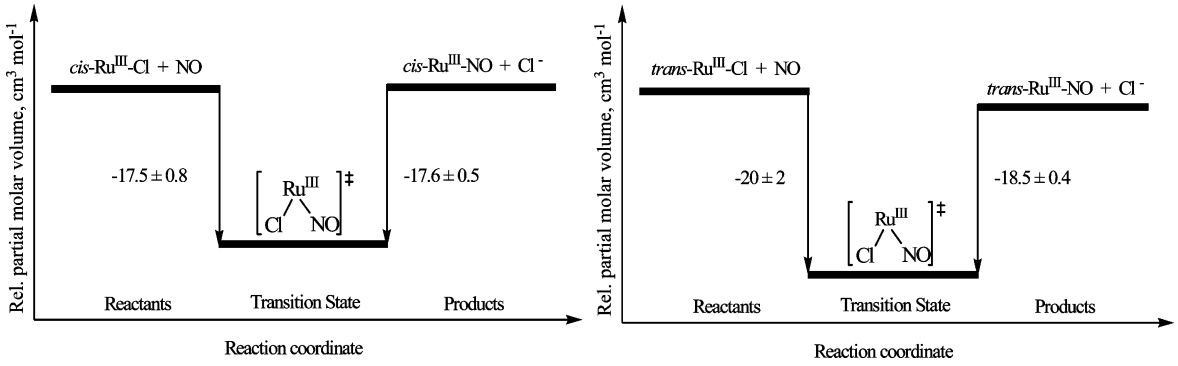

Figure 4. Volume profiles for the reversible binding of NO by *cis*-$[Ru(terpy)(NH_3)_2Cl]^{2+}$ and *trans*-$[Ru(terpy)(NH_3)_2Cl]^{2+}$.

The equilibrium constants can be calculated to be $K_1 = k_1/k_{-1} = 6371$ and 3520 M^{-1} for *cis*- and *trans*-$[Ru(terpy)(NH_3)_2Cl]^{2+}$, respectively, keeping in mind that k_{-1} includes the chloride concentration term for the reverse reaction. Although the *trans* isomer exhibits the higher rate constant for the forward reaction, the thermodynamic stability of the NO complex is in favor of the *cis* isomer.[40]

Furthermore, we suggest no conformational changes during the displacement of Cl^- by NO and vice versa. As the product of the first, fast reaction step, we propose the formation of a six-coordinate complex (see Schemes 2 and 3) in which NO is bound to Ru^{III} formally as NO^0. Thus, in the *cis* isomer NO is coordinated in the axial site, whereas in the *trans* isomer NO is coordinated in the equatorial plane, i.e., in-plane with the strong π-accepting terpy ligand. The volumes of activation for the forward and reverse reactions are so similar that the overall reaction volume for the first reaction step is close to zero[41] (see volume profiles in Figure 4). No formal change in redox state is suggested to accompany these reactions, i.e., merely ligand substitution on Ru^{III}(terpy) according to an associative mechanism.

Second Reaction Step. The second reaction step indicates a quite different behavior for both complexes. For the *trans* isomer, no dependence of the observed rate constant on [NO] was observed. In the case of the *cis* isomer, however, the observed rate constant showed a linear dependence on [NO] (Figure S12), and the reported activation parameters (Table 2) all support an associative mechanism. The observed dependence on [NO] calls for more discussion.

Although a few examples exist in the literature where two molecules of NO participate in such an overall reaction, most examples reported so far involve a nitrite catalyzed reductive nitrosylation process and refer to ferriheme proteins or related model complexes, which exhibit a different mechanistic behavior as compared to the present systems.[42] In addition, the final product does not exhibit two ν(NO) IR stretching bands, something that would be expected since all reported {RuNO}^{6} complexes are six-coordinate mono-nitrosyl species.[4] Furthermore, from the rapid-scan measurements it is known that in the overall reaction two molecules of NO are not consumed, although an excess of NO is indeed required. As already mentioned in the Experimental Section, no formation of nitrite could be detected for this isomer. Given that one molecule of NO is already bound in the first reaction step, the second participating NO molecule must be liberated again, implying either a catalytic behavior of NO or the observed kinetics reflect a combination of rate constants. The dependence of k_{obs} on [NO] for the second reaction step can be accounted for in a number of ways: (a) The concentration of the intermediate $Ru^{III}-NO$ complex is controlled by [NO] prior to electron transfer (see reaction 3), for which the rate law is given in eq 4.

$$Ru^{III}\text{—}Cl + NO \underset{}{\overset{K_1}{\rightleftharpoons}} Ru^{III}\text{—}NO + Cl^- \quad (3)$$

$$Ru^{III}\text{—}NO \xrightarrow{k_2} Ru^{II}\text{—}NO^+$$

with

$$k_{obs} = \frac{k_2 K_1[NO]}{1 + K_1[NO]}$$

and

$$K_1 = k_1/k_{-1} \quad (4)$$

Since $K_1 = 6371$ M^{-1} at 25 °C based on the kinetic data for the first reaction step, $1 + K_1[NO] \sim K_1[NO]$ and $k_{obs} = k_2$; i.e., the rate constant should be independent of [NO], which is clearly not the case.

(b) There could be rapid aquation of the intermediate $Ru^{III}-NO$ complex prior to electron transfer as formulated in eq 5, with the corresponding rate law given in eq 6. This suggestion is based on studies that include irradiation of ruthenium nitrosyl complexes with 300−350 nm light, resulting in the prompt aquation of NO and formation of the corresponding aquaruthenium(III) complexes.[34,43−45]

$$Ru^{III}\text{—}NO + H_2O \underset{}{\overset{K_2}{\rightleftharpoons}} Ru^{III}\text{—}OH_2 + NO \quad (5)$$

$$Ru^{III}\text{—}NO \xrightarrow{k_2} Ru^{II}\text{—}NO^+$$

(40) A freshly prepared solution of the *trans* isomer promptly isomerizes with a half-life of approximately 6 h under the selected experimental conditions. All experiments were therefore performed with freshly prepared solutions.

(41) The displacement of chloride by NO involves charge creation, but the contribution of electrostriction to the activation volumes could be small and is possibly not observed in the activation volumes due to the extrapolated intercept for the back reaction.

(42) Fernandez, B. O.; Lorkovic, I. M.; Ford, P. C. *Inorg. Chem.* **2003**, *42*, 2.

$$k_{obs} = \frac{k_2[NO]}{K_2 + [NO]} \quad (6)$$

K_2 must be large compared to [NO] since a linear [NO] dependence was observed. Thus, $k_{obs} = k_2[NO]/K_2$, which could in principle account for the kinetic observations. However, $\Delta V^{\ddagger}$ for this reaction is significantly negative (see Table 2). The overall $\Delta V^{\ddagger}$ for this rate law consists of two contributions as shown in eq 7.

$$\Delta V^{\ddagger} = \Delta V^{\ddagger}(k_2) - \Delta V(K_2) \quad (7)$$

Since $\Delta V(K_1)$ is ~0 (see Table 2), it is reasonable to expect that $\Delta V(K_2)$ is also close to zero. $\Delta V^{\ddagger}(k_2)$ can in principle only be positive due to the formal reduction of Ru^{III} to Ru^{II}, which will be accompanied by a significant decrease in electrostriction, i.e., increase in partial molar volume.[46] Therefore, this suggested mechanism cannot account for the observed $\Delta V^{\ddagger}$ data.

(c) There could be an NO-induced subsequent electron transfer reaction of $Ru^{III}-NO$. The similarity between $\Delta V^{\ddagger}$ for the first and second reaction steps suggests that electron transfer in $Ru^{III}-NO$ may be induced by the coordination of a second NO molecule. The formation of a seven-coordinate intermediate or transition state could account for the very negative $\Delta V^{\ddagger}$. It is therefore suggested that NO attacks the *cis* isomer axially and displaces the *trans* NO on formally reducing Ru^{III} to Ru^{II}, for which the rate law is given in eq 8 and the suggested seven-coordinate transition state is shown in Scheme 2.

$$k_{obs} = k_2[NO] \quad (8)$$

For the *trans* isomer, no kinetic evidence for the subsequent electron transfer reaction was observed. It is therefore suggested that the in-plane arrangement of Ru^{III}(terpy)NO for this isomer favors a rapid electron transfer reaction that does not require a process induced by an excess NO in solution as in the case of the *cis* isomer. As a result of the strong π-back-bonding character of terpy, NO in the in-plane position is located ideally to reduce Ru^{III} to Ru^{II} in a rapid, not observable reaction step. This favorable arrangement apparently does not require additional NO to induce the electron transfer reaction as in the case of the *cis* isomer.

In case of the *trans* isomer, we suggest a slow nitrosyl−nitrite conversion as second reaction step succeeding the electron transfer reaction. A useful route to synthesize ruthenium nitrosyl complexes is to coordinate nitrite initially to Ru^{II} and to then convert it to coordinated nitrosyl in the presence of acid. This nitrosyl−nitro equilibrium is reversible, as shown in eq 9, and depends on the pH of the solution.[47]

$$trans\text{-}[Ru(terpy)(NH_3)_2NO]^{3+} + H_2O \rightleftharpoons trans\text{-}[Ru(terpy)(NH_3)_2NO_2]^{+} + 2H^{+} \quad (9)$$

This acid−base equilibrium was also observed in the case of *cis*-$[Ru(bipy)_2(NO)(NH_3)]^{2+}$ and $[Ru(terpy)(bipy)NO]^{3+}$ with estimated acid−base equilibrium constants of 1.6×10^9 and 2.1×10^{23} M^{-2}, respectively.[30,48] For the $[Ru(terpy)(bipy)NO]^{3+}$ complex, the pH at which the nitro and nitrosyl forms are present at equal concentrations, according to reaction 9, is 2.34 which is close to our experimental condition of pH = 2.

Facile interconversion between coordinated nitrite and nitrosyl is predicted for complexes that contain essentially Ru^{II} and coordinated NO with a high degree of positive charge.[28] The higher the electron deficit in the NO fragment, the higher will be the ν(NO) stretching frequency and also the reactivity of coordinated NO. Two recent studies[34,49] showed that IR data are a useful guide to compare the relative electrophilicity of coordinated NO.[50,51] Infrared spectral data for relevant nitrosyl complexes are summarized in Table 3. The selected complexes show NO stretching frequencies between 1895 and 1952 cm^{-1}, compatible with a nitrosonium character for the NO ligand. Two general remarks are evident. First, complexes with different axial ligands *trans* to NO show that the presence of different ligands in the coordination sphere implicates dramatic changes in the ν(NO) stretching frequency. Second, in complexes where the

Table 3. Data for ν(NO) for Selected Nitrosyl Complexes

complex	ν(NO) in cm^{-1}	ref
$[Ru(terpy)(bipy)NO]^{3+}$	1952	48
cis-$[Ru(bipy)_2(NO)(NH_3)]^{3+}$	1944	32
cis-$[Ru(bipy)_2(NO)(NH_3)](PF_6)_3$	1950	31
cis-$[Ru(bipy)_2(NO)(Cl)](PF_6)_2$	1934	26
trans-$[Ru(bipy)_2(NO)(Cl)](PF_6)_2$	1912	26
trans-$[Ru(NH_3)_4(NO)(H_2O)](SO_4)(HSO_4)$	1920	58
trans-$[Ru(NH_3)_4(NO)(H_2O)](Cl)_3$	1912	33
$[Ru(NH_3)_5(NO)](Cl)_3$	1903	57
trans-$[Ru(NH_3)_4(NO)(Cl)](Cl)_2$	1880	57
trans-$[Ru(NH_3)_4(NO)(OH)](Cl)_2$	1834	59
trans-$[Ru(terpy)(Cl)_2NO](PF_6)$	1895	27
trans-$[Ru(py)_4(NO)(Cl)](PF_6)_2$	1911	60
$[Ru(terpy)(NO)(H_2O)(NH_3)]^{3+}$	1926	this work

(43) Tfouni, E. *Coord. Chem. Rev.* **2000**, *196*, 281.
(44) A $Ru^{III}-NO^0$ intermediate is produced on irradiation of Ru^{II}–NO^+, involving a formal electron transfer from the metal to the nitrosyl ligand, which is followed by a rapid aquation reaction. A mechanism was suggested whereby excitation of a $t_2 \rightarrow \pi^*$ (NO) transition (300−400 nm) results in the expulsion of NO. The reaction was reported to be reversible.
(45) Works, C. F.; Ford, P. C. *J. Am. Chem. Soc.* **2000**, *122*, 7592. Works, C. F.; Jocher, C. J.; Bart, G. D.; Bu, X.; Ford, P. C. *Inorg. Chem.* **2002**, *41*, 3728.
(46) The reaction volumes for various $[RuX]^{3+/2+}$ couples (with X = $(NH_3)_6$, $(H_2O)_6$, and $(en)_3$) were determined in aqueous solution using high-pressure cyclic voltammetry. The reaction volume, ΔV, was reported to be strongly positive in the case of ammine complexes, which was mainly assigned to the decrease in electrostriction on reduction of the complex. Sachinidis, J. L.; Shalders, R. D.; Tregloan, P. A. *Inorg. Chem.* **1996**, *35*, 2497.
(47) No pH dependence study was performed for this step, although it should be pH sensitive. At lower pH, the interconversion between coordinated nitrosyl to nitrite should be faster, but the experimental work was already performed at pH = 2. At higher pH, this interconversion should be slower, but the reaction could involve the attack of NO on the deprotonated ammine complex as in the case of the ammine complexes which results in quite a different product.
(48) Murphy, W. R. Jr.; Takeuchi, K. J.; Meyer, T. J. *J. Am. Chem. Soc.* **1982**, *104*, 5817.
(49) Roncaroli, F.; Ruggiero, M. E.; Franco, D. W.; Estiú, G. L.; Olabe, J. A. *Inorg. Chem.* **2002**, *41*, 5760.
(50) McCleverty, J. A. *Chem. Rev.* **1979**, *79*, 53.
(51) Bottomley, F. *Acc. Chem. Res.* **1978**, *11*, 158.

nitrosyl ligand is located *trans* to a terpy or bipy ligand, the ν(NO) stretching frequency is even higher.

IR data for the nitrosyl complex of the *cis* isomer are in good agreement with those of the listed nitrosyl complex (Table 3). For the *trans* isomer, which corresponds to the *cis* complexes (NO is located *trans* to a terpy or bipy ligand), the ν(NO) stretching frequency following NO coordination and subsequent reduction is not available. But it seems reasonable to expect a ν(NO) stretching frequency in the region of *cis*-$[Ru(bipy)_2(NO)(NH_3)]^{3+}$ with $\nu(NO) = 1944$ (1950) cm^{-1} and $[Ru(terpy)(bipy)NO]^{3+}$ with $\nu(NO) = 1952$ cm^{-1}. Comparing the corresponding *trans*- and *cis*-$[Ru(bipy)_2(NO)(NH_3)]^{3+}$ complexes, the *trans* isomer exhibits its ν(NO) mode in a frequency range 22 cm^{-1} lower than the *cis* isomer, an approved feature[26,52] also expected for our complexes. The expected higher ν(NO) stretching frequency for the *trans* isomer provides a sound basis for reaction 9 to occur in this particular case, which we consider to be the second reaction step for the *trans* isomer.

Third Reaction Step. As already mentioned above, the final reaction step in the overall process shows no dependence on NO. Since the large excess of solvent water presents the only potential nucleophile, we suggest that the final step involves a slow aquation reaction. The synthesized isomers are rather novel since they are between simple ammine complexes and highly substituted polypyridyl systems, for which nearly no substitution data are available. On comparing aquation reactions of Ru^{III} and Ru^{II} ammine complexes, marked differences in their mechanistic behavior are observed. Several studies on Ru^{III} centers support evidence for an associative substitution mechanism (I_a or A).[25,53,54] In contrast, Ru^{II} complexes are significantly more labile, and substitution occurs via a dissociative mechanism (I_d or D).[55,56] The large and positive activation volumes $\Delta V^{\ddagger}$ found for the final reaction step for both isomers support a dissociative mechanism on the basis that the formal oxidation state of the metal ion is +2.

The final aquation reaction of both isomers requires more discussion with respect to the nature of the leaving group. In the *cis* isomer, two molecules of ammonia remain in the *cis* arrangement following the second reaction step (see Scheme 2). In ruthenium-nitrosyl complexes, it has been found that the NO group has a very strong labilizing effect on the group in the *trans* position.[57] In linear Ru−NO complexes, NO is such a good π-acceptor and poor σ-donor that NO and the *trans* ligand compete for the same orbitals. Since water is generally not considered to be a π-bonding ligand, it is quite likely that it will substitute the ammonia molecule *trans* to the NO group.

For the *trans* isomer, the observed second and third reaction steps are ascribed to slow subsequent processes (see Scheme 3). From the nitrite test (see Experimental Section), we are confident to conclude that coordinated nitrite undergoes an aquation reaction. The $\Delta V^{\ddagger}$ data for the third reaction step is in agreement with dissociation of nitrite. This step may be acid-catalyzed and involve the release of neutral HONO, which should be in close agreement with the release of NH_3 in the case of the *cis* isomer, especially in terms of volume changes.

Conclusions

In summarizing the overall reactions of *cis*- and *trans*-$[Ru(terpy)(NH_3)_2Cl]^{2+}$ with NO, a complex multistep reaction sequence was observed. The first step for both isomers includes a rapid reversible formation of a $Ru^{III}-NO^0$ intermediate, which is in good agreement with the general substitution behavior of Ru^{III} complexes and proceeds according to an associative mechanism. Both isomers show the expected enhanced reactivity in comparison to the $[Ru(NH_3)_5Cl]^{2+}$ complex, as a result of the higher π-acceptor ability of the terpy ligand and the stronger electrophilic character of the Ru center. The *trans* isomer exhibits a higher rate (by a factor <3) than the *cis* isomer, which is quite reasonable in light of the more electrophilic Ru^{III}(terpy) center. This primary step is followed by a fast electron transfer reaction. In case of the *cis* isomer, this electron transfer occurs only through the assistance of a second NO molecule. The fact that this second reaction step is characterized by a transition state with a strongly associative character supports our suggestion of an NO-induced subsequent electron transfer process. Since substitution on Ru^{III} is known to occur via an associative mechanism and on Ru^{II} via a dissociative mechanism, the oxidation state of the metal center following the first reaction step must still be +3. For the *trans* isomer, no kinetic evidence for subsequent electron transfer was found, but on going to the third reaction step, the large and positive volume of activation indicates that electron transfer must have occurred before. We pointed out that, also for the *trans* isomer, three reaction steps are obtained by fitting the kinetic traces at 25 °C, but the second and third steps become so similar in rate that they could not be separated kinetically. We suggest that the nitrosyl−nitro interconversion occurs during the second reaction step and is caused by the high degree of positive charge on coordinated NO^+ in this isomer. Finally, the third reaction step for both isomers can be characterized as an aquation process. In case of the *cis* isomer, the NO group shows a strong *trans* labilization effect and therefore causes the displacement of the *trans* ammine ligand. For the *trans* isomer, we suggest an acid-catalyzed dissociation of HONO.

(52) Pell, S.; Armor, J. N. *Inorg. Chem.* **1973**, *12*, 873. Kamata, Y.; Kimura, T.; Hirota, R.; Miki, E.; Mizumachi, K.; Ishimori, T. *Bull. Chem. Soc. Jpn.* **1987**, *60*, 1343.
(53) Fairhurst, M. T.; Swaddle, T. W. *Inorg. Chem.* **1979**, *18*, 3241.
(54) Broomhead, J. A.; Kane-Maguire, L. *Inorg. Chem.* **1968**, *7*, 251.
(55) Taube, H. *Comments Inorg. Chem.* **1981**, *1*, 17. Swaddle, T. W. *Coord. Chem. Rev.* **1974**, *14*, 217.
(56) Grundler, P. V.; Laurenczy, G.; Merbach, A. E. *Helv. Chim. Acta* **2001**, *84*, 2854. Aebischer, N.; Sidorenkova, E.; Ravera, M.; Laurenczy, G.; Osella, D.; Weber, J.; Merbach, A. E. *Inorg. Chem.* **1997**, *36*, 6009.
(57) Mercer, E. E.; McAllister, W. A.; Durig, J. R. *Inorg. Chem.* **1966**, *5*, 1881.
(58) Emel'yanov, V. A.; Virovets, A. V.; Baidina, I. A.; Gromilov, S. A.; Belyaev, A. V. *Inorg. Chem. Commun.* **2001**, *4*, 33.
(59) Schreiner, A. F.; Lin, S. W.; Hauser, P. J.; Hopcus, E. A.; Hamm, D. J.; Gunter, J. D. *Inorg. Chem.* **1972**, *11*, 880.
(60) Goodman, M. S.; DeMarco, M. J.; Haka, M. S.; Toorongian, S. A.; Fridmann, J. *J. Chem. Soc., Dalton Trans.* **2002**, 117.

Altogether, we investigated a system of two isomeric complexes that again shows a surprisingly fast reaction with NO, as already observed for the $[Ru^{III}(NH_3)_5X]^{(3-n)+}$ systems ($X^{n-} = NH_3$, H_2O, Cl^-).[12] For the pentaammine systems, an associative substitution mechanism coupled to a concerted electron transfer step was proposed.[12] On one hand, the investigated complexes here exhibit an enhanced reactivity for the ligand substitution process, but on the other hand, the electron transfer reaction seems for some reason inhibited, since in the case of the *cis* isomer a second NO molecule is apparently required to induce the reduction of the metal center. The one-step process observed for the pentaammine system is split into two reaction steps for the studied terpy complexes with an equilibrium-dependent formation of the $Ru^{III}-NO^0$ complex and a subsequent electron transfer reaction. The overall redox reaction is governed by a higher equilibrium constant which shows up mainly in the complex-formation step. The *cis*−*trans* effects in substitution reactions of octahedral ruthenium complexes have received little attention up to now. Evidently, the pathways differ more on the basis of the electrophilic Ru^{III}(terpy) center in the case of the *trans* isomer. The reaction patterns observed seem to be solely controlled by the influence of the terpy ligand in the studied isomers.

Acknowledgment. The authors gratefully acknowledge financial support from the Deutsche Forschungsgemeinschaft, Fonds der Chemischen Industrie, and the Max-Buchner Forschungsstiftung.

Supporting Information Available: Kinetic traces recorded for the overall reactions for both isomers. Plots of kinetic and thermodynamic parameters for the first, second, and third steps in the reactions of *cis*- and *trans*-$[Ru(terpy)(NH_3)_2Cl]^{2+}$ with NO. The molecular structure of *trans*-$[Ru(terpy)(NH_3)_2Cl](PF_6)_2 \cdot 2H_2O$ with a summary of crystal data, structure refinement parameters, and selected bond distances and angles. Crystallographic information in CIF format. This material is available free of charge via the Internet at http://pubs.acs.org.

IC0350685